energy&fuels

Article

pubs.acs.org/EF

Influences of the Initial Ignition Energy on Methane Explosion in a Flame Deflagration Tube

Mohammed J. Ajrash,[†] Jafar Zanganeh,*[,†] and Behdad Moghtaderi[†]

[†]The Frontier Energy Technologies Centre, Chemical Engineering, School of Engineering, Faculty of Engineering & Built Environment, University of Newcastle, Callaghan, NSW 2308, Australia

ABSTRACT: It was observed that the initial ignition energy influences the flame deflagration characteristics of methane explosions. This distinct behavior has been noticed by a number of scholars, and in our laboratory scale explosion chamber recently. However, the flame traveling behavior has not been adequately clarified in industrial scale flame deflagration tube (FDT). This experimental work investigates methane flame deflagration and varied initial ignition in a large scale FDT (30 m long) facilitated at University of Newcastle, Australia, to comprehensively investigate methane flame deflagration behavior. The initial ignition energy was delivered by three alternative chemical ignitors' energies, which were 1, 5, and 10 kJ. The results of the study revealed the notable influences of the initial ignition energies on the flame deflagrations, over pressure rises, and pressure wave velocities along the FDT. When the initial ignition energy was increased from 1 kJ to 10 kJ, the maximum over pressure rises increased by 45% and 56%, respectively, for the 7.5% and 9.5% methane concentrations. For a 9.5% methane concentration, the increased ignition energy enhanced the pressure wave velocity from 130 $m{\cdot}s^{-1}$ to 359 $m{\cdot}s^{-1}$ and enhanced the flame deflagration velocity from 105 $m{\cdot}s^{-1}$ to 179 $m{\cdot}s^{-1}$.

1. INTRODUCTION

The hazards of methane explosions and flame deflagrations still represent a threat for chemical plants, mining tunnels, pipes, and other extractive and processing concerns. Accidental fires in the process industries can cause enormous losses in life and capital.[1−4] One of the challenges is to eliminate and reduce the consequences of accidental fires and explosions in pipes. To achieve that goal, accurate data concerning large scale setups is required to understand the characteristics of methane explosions in pipes.[5]

The hazards of gas explosions in pipes was first highlighted in the last century by a number of scholars.[6,7] They observed that the pressure in a tube develops and eventually leads to a rapid pressure rise, commonly termed a detonation. The properties of methane flame deflagration in pipes were first investigated by Mason and Wheele.[8,9] They used a 5 m long laboratory scale tube of 20 mm diameter. They noticed that the flame deflagration velocity increases as the flame reaches the end of the tube. Phylaktou (1990)[10] investigated methane explosions and the resultant flame deflagrations in a vertical laboratory scale pipe. He found that the pressure rise may reach 6.9 bar at some point during the flame deflagration. Additionally, he observed that the flame does not deflagrate at a constant velocity.[10] In a 30 m detonation tube, the behaviors of static and dynamic pressures were examined as functions of the methane volume.[11] The goal was achieved by using a varied length per diameter ratio (L/D) of FDT. The authors claimed that the methane volume had no effect on the static and dynamic pressures when the tube was open at one end. Qingzhao et al.[12] used a closed laboratory scale explosion tube to investigate the characteristics of 9.5% methane explosions ignited by a 10 kJ initial ignition energy (IIE). The authors observed that the reflected pressure wave could rupture and extinguish the flame. Another series of large scale detonation tube experiments have previously been conducted to address the locations and properties of methane explosions, which eventually end up as detonation phenomena.[13−22] Other scholars have investigated the influences of other factors on methane ignition and flame propagation, such as the initial conditions.[23−25] A number of researchers have highlighted explosion characteristics and the effects of IIE on the flammability limit of methane. Zabetakis et al.[26] tabulated the flammability limits of methane at atmospheric conditions. The results were based on a small scale experimental setup. Hertzberg et al.[27] used a 20 L (liter) explosion vessel to investigate the flammability limits and pressure rise rates of methane under variable IIEs. Herzberg et al. concluded that the pressure rise of a methane explosion (at the stoichiometric air concentration) initiated by high IIE is lower than the explosion initiated by a low IIE.[27] Cashdollar et al.[28] used 20 and 120 L explosion vessels to thoroughly analyze the flammability limits of methane and other hydrocarbon gases. The scholars proved that the IIE could extend the methane and hydrocarbon gas flammability limits. Bai et al.[29] studied the flame deflagration and pressure profiles of methane and a hybrid mixture (methane-coal dust) employed in a 10 m^3 cylindrical explosion chamber (3.5 m long, 2 m diameter). The findings for the methane air mixture showed that the 40 mJ ignitor limited the methane ignition by between 5% and 13%, and limited the maximum pressure rise to between 5% and 13%, at a distance according to the methane concentration. The duration of the ignition spark has been explored by Zhang et al.,[30] who employed 5 and 20 L explosion vessels to discuss the influence of explosion chamber volume on explosion characteristics. The authors showed that the explosion characteristics are slightly

Received: December 22, 2016
Revised: April 30, 2017
Published: May 1, 2017

DOI: 10.1021/acs.energyfuels.6b03375
Energy Fuels XXXX, XXX, XXX−XXX

Table 1. Most Recent And Relevant Literature That Deals With Methane Configration

author	experimental setup	dimension	IIE	methane concentration in air	max pressure (bar)	max flame velocity (m/s)
Ajrash et al., 2017[34]	open end FDT (12 m reactive section)	30 m long, 0.5 m diameter	50 mJ	5−7.5%	2.1	132
Ajrash et al., 2017[33]	open end FDT (3,6,12, and 25 m reactive section)	30 m long, 0.5 m diameter	50 mJ	1.25−15%	3.75	170
Mitu et al., 2017[35]	spherical vessel	0.52 L	Spark (3−5 mJ)	7−12%	6.1	
Ajrash et al., 2016[32]	open end FDT (5 m reactive section)	30 m long, 0.5 m diameter	50 mJ	2.5−6%	0.53	53
Wei et al., 2009[11]	open end FDT (10 m reactive section)	30 m long, 0.5 m diameter		6−10%	2.3	
Tang et al., 2014[36]	cylindrical closed vessel	0.18 m diameter, 0.21 m length	45 mJ	stoichiometric	5.8	
Gieras et al., 2006[37]	closed cylindrical vessel	40 L volume, 0.34 m diameter	electrical spark	4.1−17.2%	7.9	
Kindracki et al., 2007[38]	horizontal closed tube	1.325 m long, 0.1285 m diameter	electrical spark	7%	5.4	
				9.5%	6.4	
Kindracki et al., 2007[38]	vertical closed tube	1.325 m long, 0.1285 m diameter	electrical spark	7%	4.2	
				9.5%	6.2	
Bader et al., 1984[39]	closed vertical tube	3 m	electrical spark	7.5%		0.62
				9.5%		1.05
	closed horizontal tube			7.5%		0.55
				9.5%		0.98
Cao et al., 2017[40]	closed vertical chamber	0.91m*0.15 m*0.15 m	electrical spark	9.5%	5.6	8.4
Jiang et al., 2013, 2016[41]	open end duct	0.08m *0.08 and 21 m length	electrical spark 2 J	9.5%	0.42	131 0.1
Zhang et al., 2014[42]	open end duct	0.4 m* 0.4 and 10 m length		9.5%		92
Liu et al., 2013[43]	open end FDT	30.8 m length and 0.199 m diameter	explosion of 7m stoichiometric epoxypropane mist/air	9.5%	120 (quasi DDT)	2100 (quasi DDT)

affected by the IIE duration (60.5 μ s - 10.6 μs) and the weak ignition energy (54 mJ - 430 mJ). Additionally, the wall temperature of the 20 L explosion chamber was lower than the temperature of the 5 L explosion chamber wall for the same explosion conditions. Ajrash et al.[31] used a 20 L explosion chamber to investigate the pressure rises of pure methane and hybrid mixtures at lean methane concentrations. Three different IIEs were used (1, 5, and 10 kJ chemical ignitors). The results showed that there was no significant pressure rise when the explosion was initiated by a 1 kJ ignitor at a 5% methane concentration, however, the mixture became flammable when using a 5 kJ ignitor as the IIE. The results clearly showed the explosive and nonexplosive regions for the methane and methane-coal dust hybrid mixtures according to IIE. Additionally, the flame deflagration was also affected by the IIE, where the deflagration index increased from 1 bar·m·s^{-1} to about 4 bar·m·s^{-1}, when a 5 kJ, rather than a 1 kJ, IIE was being used. The previous results investigated the role of the IIE and the explosion characteristics for a closed chamber (confined space), however,[32] it also showed the influence of IIE in a 1 m^3 cylindrical open end tube (semiconfined space). The investigation went beyond the explosion characteristics by discussing the influences of the IIE on the flame front behavior and pressure wave speed. Initial combustion for a 6% methane concentration started 35 ms (ms) earlier, and the flame was faster by about 7 m·s^{-1} when employing a 10 kJ IIE instead of a 1 kJ IIE. In other experimental work conducted by Ajrash et al.,[33] the ignition condition was fixed and delivered by the explosion of a 9.5% methane concentration (initiated by 50 mJ chemical ignitors) in the first 2 m of a 30 m long FDT. The author indicated that flame deflagration velocity is highly dependent on the initial ignition energy introduced to the reactive sections, especially for low methane concentrations (i.e., below 7.5% methane).

The findings of the previous literature indicate that the level of initial ignition energy significantly impacts on the flame and explosion phenomena, and also reduces the lower flammability limit of the fuel. While the geometry and volume of an experimental apparatus plays an important role in explosion characteristics, the majority of the past studies have been conducted on small volume (e.g., 20 L) spherical shape geometries. Also, those studies have not clarified how the initial ignition will impact on the flame deflagration. Therefore, it is essential to gain a better understanding of flame deflagration and explosions, particularly in large scale geometry vessels. This will then assist in determining the correlation between the pressure rise and initial ignition energy associated with the larger geometry. Table 1 shows the most relevant and recent works to have employed the FDT. The literature review revealed a lack of data on methane explosions and knowledge of their consequences in FDT. The current study, however, aimed to examine the significance of the IIE of a methane explosion in an FDT. This study first addressed the dynamic and static pressures of methane in order to assist in measuring the expected damage levels. Additionally, the pressure waves were investigated along the FDT as a function of the IIE. The pressure wave profiles examined the forms of both the static pressure and the velocity of the pressure wave. Finally, the influence of IIE on flame deflagration is elucidated in terms of the flame intensity signal and velocity.

DOI: 10.1021/acs.energyfuels.6b03375
Energy Fuels XXXX, XXX, XXX−XXX

2. EXPERIMENTAL SETUP

2.1. FDT and Diagnostics. The FDT was 30 m long and had a 0.5m diameter (see Figure 1). The pressure wave value and flame front

Figure 1. FDT at University of Newcstle, Australia.

velocity were measured and tracked by 33 pressure transducers which were mounted to the system at the rate of three transducers per section. The pressure transducers can provide readings of up to 60 bar, with an error reading of less than 0.25%, and a response time of <0.1 ms. The photodiodes had the following specifications: an active area of 0.8 mm^2, a wavelength range of 200−1100 nm, a rise time of 1 ns, and a bias voltage of 10 V.

The reactive section is presented in sections 1, 2, and 3 (see Figure 3). Sections 3 to 11 represent the nonreactive system (the gray sections in Figure 3). A blowing system at the beginning of the tube was used to refresh the air inside the tube. A pyrometer measured the temperature (400−2000 °C) of the reactive system through a sapphire window. A high speed color camera (type Phantom 4) was set at 2000 fps and a standard video camera was located at the beginning of the FDT (type Bazlar, set at 255 fps) (see Figure 2).

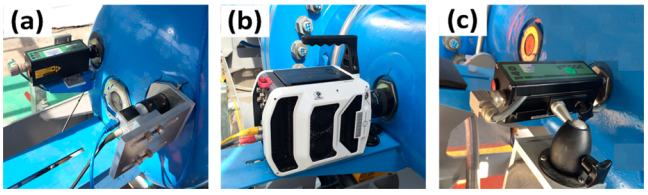

Figure 2. Flame monitoring equipment: (a) pyrometer and video camera mounted at the beginning of tube, (b) high speed camera mounted at the side view of section 1, and (c) pyrometer mounted at the side view of section 6.

2.2. Gas Mixture. The homogeneity of the methane air mixture was achieved by two circulation systems along the tube. Each circulation system consisted of a blower, with volumetric flow rates of 720 L/min and 1900 L/min for the first and second circulation blowers, respectively, four pneumatic valves, a methane monitor, two flame arrestors, and a rotameter (see Figure 3).

For each system there was a methane line connected to a methane cylinder via two pneumatic valves and a mass control flowmeter.

2.3. Initial Ignition Energy (IIE). A chemical ignitor with three different energy levels of 1, 5, and 10 kJ was employed as the IIE, the ignitors lactated at the beginning of the FDT (see Figure 4). Instrument air was used to minimize the effects of moisture, and any impurities associated with the air, on the methane mixtures' explosion properties. The explosion characteristics, pressure wave velocities, and flame velocities were investigated for three methane−air mixture concentrations (5, 7.5, and 9.5%).

2.4. Procedure. The system was designed to be operated from a control room located 30 m from the explosion chamber. To conduct the test, the system was first purged with fresh air by activating the purging system (an air blower and two pneumatic valves). Then the ignitor (1, 5, or 10 kJ) was placed at 20 cm distance from the beginning of the FDT. The sealing system consisted of a pneumatic valve, manual valve, and portable pump. The next step after sealing off the sections was to evacuate the site. All the sensors were activated at the time of ignition for the measurement of the pressure, temperature, and detection of the flame. The data was automatically saved on the logging and control computer. Finally, the system was purged with fresh air after the completion of each test. Table 2 shows the nominal and measured methane concentration as well as the IIE and temperature used in this study.

3. RESULTS AND DISCUSSION

3.1. Pressure Rise. The pressure rise of an explosion is an essential factor used in the design of chemical plant equipment. The pressure rise is important for the determination of three design aspects: first, the constructed system should be able to contain the expected pressure rise; second, the destruction can be reduced by using an appropriate control method (i.e., pressure venting); and finally, it is needed to determine the risk level.[44] In the current configuration of the DT, the flame deflagrates from the closed end toward the open end. During the flame deflagration phase, the combustion products exert a side pressure which is vertical to the flame direction (static pressure). Another pressure forms ahead of the flame (dynamic pressure). The dynamic pressure is also important for calculating the fluid velocity ahead of the flame. Although the application of static or dynamic pressures would give some indications of the exerted pressure on a structure, it would not, however, provide the actual figure. Therefore, to determine the actual pressure imposed on a structure caused by an explosion, it is necessary to consider the total pressure (stagnation pressure) in calculation. Knowledge of stagnation pressure can also contribute to estimating the actual pressure wave force which is exerted on the fire mitigation countermeasures and their accessories. The maximum pressure in this study is measured along the tube, and the dynamic and stagnation pressures are measured close to the end of the tube, for all methane concentrations. The experimental work was repeated once for each data point. Figure 5 shows an acceptable consistency between the results with a slight variation. This variation can be attributed to the full scale accuracy (0.05%) of the methane monitor reading and slight fluctuations in the initial conditions (e.g., temperature). The maximum pressures recorded for the explosions of 5, 7.5, and 9.5% methane concentrations are shown in Figure 5. The figure displays the maximum pressure rise related to the IIE. The results first showed that the pressure rise for a 9.5% methane concentration was about twice the maximum pressure rise as for a 7.5% methane concentration, regardless of the IIE. Additionally, the results indicated that the IIE has a significant impact on the maximum pressure rise along the FDT. For a 7.5% methane concentration, the maximum pressure rise of the flame deflagration increased by about 45% as the IIE increased from 1 kJ to 10 kJ. However, at a 9.5% methane concentration, the maximum pressure rise increased by 56% as the IIE increased from 1 kJ to 10 kJ.

Using a 5 kJ chemical ignitor instead of a 1 kJ ignitor increased the maximum pressure rise by 36% and 23% for 7.5% and 9.5% methane concentrations, respectively (see Figure 5). At 5% methane, no pressure rise was observed for both 1 kJ and 5 kJ ignitors, however, when using a 10 kJ ignitor a slight increase in the pressure value (0.17 bar) was observed. The static and dynamic pressures were measured at the last section of the FDT (section 11). Two pitot tubes where employed to

DOI: 10.1021/acs.energyfuels.6b03375
Energy Fuels XXXX, XXX, XXX−XXX

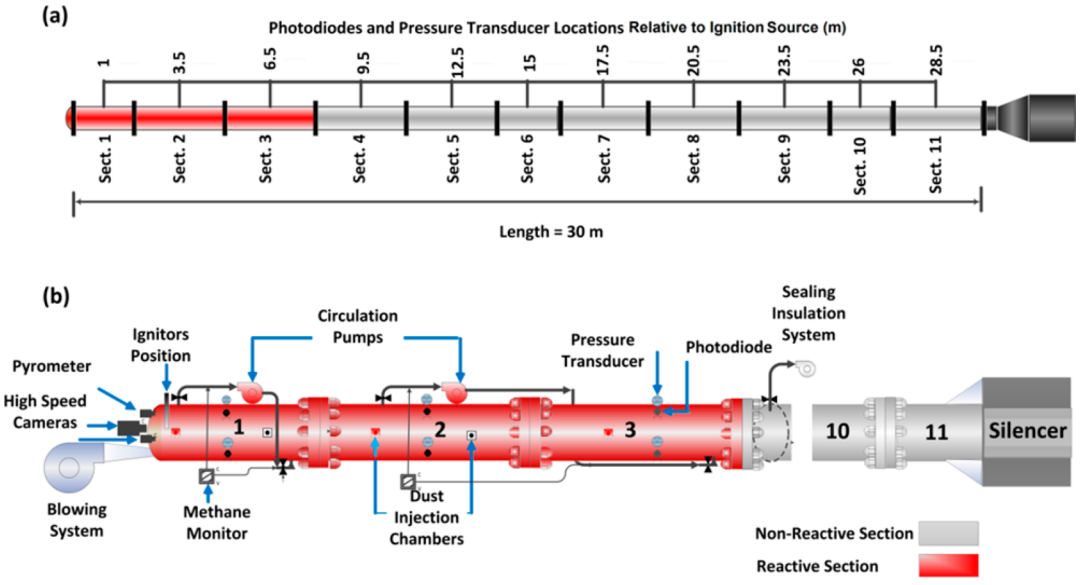

Figure 3. Components of the FDT at the University of Newcastle.

Figure 4. Chemical ignitors used in this work: (a) 1 kJ, (b) 5 kJ, and (c) 10 kJ.

Table 2. Test Runs Matrix and Conditions

test no.	methane conc.	IIE (kJ)	first methane monitor	second methane monitor	initial temp. inside FDT
#1	5%	1	4.87	4.97	27
#2		repeat	5.1	4.96	24
#3		5	5.08	5.11	28
#4		repeat	5.24	5.11	24
#5		10	5.09	4.83	27.6
#6	7.5%	1	7.7	7.52	25
#7		repeat	7.65	7.38	29
#8		5	7.51	7.52	23
#9		repeat	7.63	7.52	33
#10		10	7.52	7.51	24
#11		repeat	7.66	7.5	22
#12	9.5%	1	9.55	9.5	30
#13		repeat	9.85	9.6	23
#14		5	9.8	9.48	31
#15		repeat	9.74	9,47	24
#16		10	9.7	9.63	27
#17		repeat	10	9.48	24

measure the dynamic pressure, and the static pressure was measured by reading the pressure transducers mounted radially around the tube inside the surface in each section. The stagnation pressures were calculated as follows:

$$P_{Stag} = P_{st} + P_{Dyn} \quad (1)$$

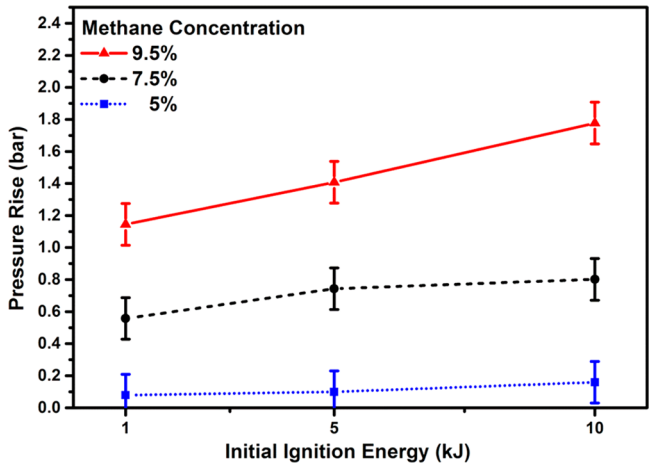

Figure 5. Maximum pressure rise for the explosions of 7.5% and 9.5% methane concentrations as a function of the IIE.

Where P_{Stag} is the stagnation pressure, $P_{st,}$ is the static pressure, and P_{Dyn} is the dynamic pressure.

For the explosion of the 7.5% methane concentration, the stagnation, dynamic, and static pressures are illustrated in relation to the IIE in Figure 6. The results show that the dynamic pressure was higher than the static pressure for all three IIEs. The influence of the IIE was most obvious on the stagnation pressure. The maximum stagnation pressure (0.9 bar) was achieved when using 10 kJ IIE (see Figure 6).

For the explosion of the 9.5% methane concentration, the stagnation, dynamic, and static pressures are illustrated in relation to the IIE in Figure 7. The results for the 9.5% methane concentration, as compared to the 7.5% concentration, show that the gap between the dynamic pressure and the static pressure increased. This may be attributed to the fact that at a 9.5% methane concentration, the combustion products behind the flame exert a higher pressure on the axial direction of the flame deflagration than a 7.5% methane concentration. The influence of increasing the IIE on the static pressure was more pronounced. When the IIE was increased 5-fold, from 1 kJ to 5 kJ, the static pressure increased by 69%. However, when the IIE

DOI: 10.1021/acs.energyfuels.6b03375
Energy Fuels XXXX, XXX, XXX−XXX

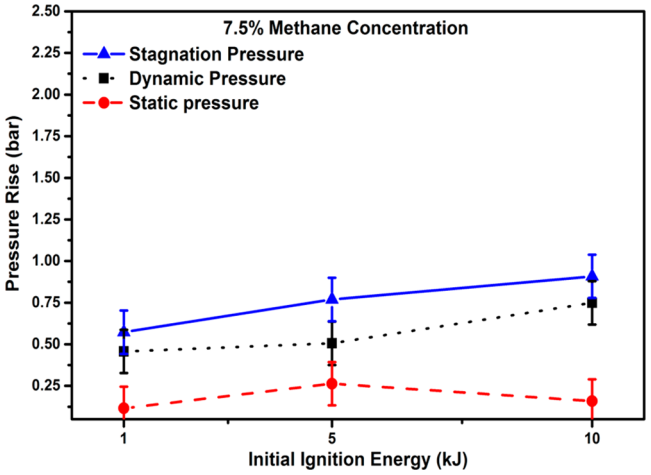

Figure 6. Stagnation, static, and dynamic pressures for 7.5% methane concentration at section 11.

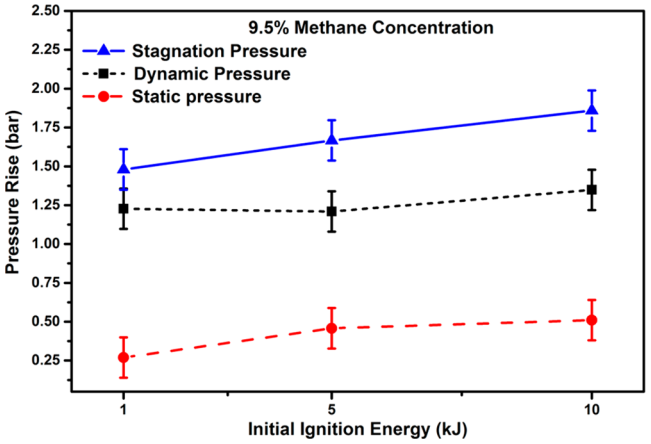

Figure 7. Stagnation, static, and dynamic pressures for 9.5% methane concentration.

was increased 2-fold, from 5 kJ to 10 kJ, the static pressure only increased by 10%. The dynamic pressure had an almost fixed value when increasing the IIE from 1 kJ to 5 kJ, and the boost in the dynamic pressure was more pronounced when the IIE was increased from 5 kJ to 10 kJ. The variations in both the dynamic and static pressures were reflected in the stagnation pressure (see eq 1). The stagnation pressure was clearly boosted by increasing the IIE. The stagnant pressure values increased by about 12% when increasing the IIE from 1 kJ to 5 kJ, and had a similar boost when increasing the IIE from 5 kJ to 10 kJ (see Figure 7). Finally, neither dynamic nor static pressures were detected at the end of the FDT for a 5% methane concentration at all ranges of initial ignition energies.

3.2. Pressure Wave Tracking. An effective approach to pressure rise should take into consideration the expected pressure development during the flame deflagration. The pressure wave is mainly produced by the expansion of combustion product gases behind the flame. The velocity of the deflagration flame may be fully developed or self-sustaining, which may cause high pressure gases behind the flame. These gases are formed at a certain time, boosting the pressure rise in the pipes. The flame velocity and/or the burning rate in the horizontal pipes is dependent on a number of factors, such as the Length/Diameter (l/d) ratio, pipe roughness, the flammable gas's properties, initial conditions, and the ignition energy. In the current study, there were two variables considered, the percentage of the methane and the IIE. To get accurate insights into the pressure wave profile properties of methane explosions in pipes, this section discusses both the pressure rise profiles and the pressure wave velocities for 7.5% and 9.5% methane concentrations ignited under three IIEs (1, 5, and 10 kJ). For this section and Section 3.3 the test runs numbered 6, 8,10,13,14, and 16, corresponding to Table 2, were considered in the analysis. The average variation of pressure values between the first and repeat runs was in the range of 2% and 1.15% for 7.5% and 9.5% methane concentrations, respectively. However, the average variation in terms of flame velocity between the first run and the repeat run was in the range of 2% and 8% for 7.5% and 9.5% methane, respectively. The variation between the first run and the repeat run is reasonable, and is due to the variations of the initial temperature as well as slight variations in the methane concentration.

3.2.1. Pressure Wave Values. The pressure wave values represented by the pressure rises are shown in Figure 8. Figure 8a shows the methane (7.5% and 9.5% concentrations) pressure rise profiles initiated by a 1 kJ IIE. For the 7.5% methane, a pressure wave was generated at a value between 0.29 and 0.32 bar, then at 20.5 m it was noted that the pressure increased up to 0.38 bar, and the maximum pressure rise was recorded at 26 m. At the stoichiometric methane concentration (9.5%), the pressure wave traveled at a pressure rise between 0.86 and 0.75 bar, then dramatically developed to 1.05 bar at 15 m, and the maximum pressure rise was achieved at 23.5 m. The ratio of the highest to lowest pressure rise values was 35%.

Figure 8b shows the methane (7.5% and 9.5% concentrations) pressure rise profiles initiated by a 5 kJ IIE. For the 7.5% methane concentration, the pressure wave traveled at a value between 0.48 and 0.4 bar, then at 15 m the pressure increased up to 0.5 bar, and the maximum pressure rise was recorded at 20.5 m. At the methane stoichiometric concentration, the pressure wave traveled at a pressure rise between 1.02 and 1.08 bar, then at 17.5 m the pressure rise increased to 1.37 bar, and the maximum pressure rise occurred at 20.5 m. The ratio of the highest to lowest pressure rise values was also 35%. Figure 8c shows the methane (7.5% and 9.5% concentrations) pressure rise profiles initiated by a 10 kJ IIE. For the 7.5% methane concentration, the pressure wave traveled at about 0.52 bar, then at 12.5 m it was marked that the pressure developed to 0.8 bar, and the maximum pressure rise was recorded at 20.5 m. At the methane stoichiometric concentration, the pressure wave traveled at a pressure rise between 0.86 and 1.3 bar, then at 15 m the pressure rise dramatically increased to 1.78 bar and the pressure continued to increase, reaching the maximum value at 20.5 m. The ratio of the highest to lowest pressure rise values was 66%.

Subsequent to this experimental investigation, the pressure wave was calculated using the following equations. Results obtained for pressure waves from these equations are consistent with the experimental data and show a similar pattern.

$$PR = y_o + \frac{A}{\sqrt[6.5]{\frac{\pi}{4\ln(2)}}} e^{-4\ln(2)(x-xc)/42.25} \quad (2)$$

Where x, is the distance from the ignition source, y_o, A, and xc could be solved according to initial ignition energy from 1 kJ to 10 kJ as follows

DOI: 10.1021/acs.energyfuels.6b03375
Energy Fuels XXXX, XXX, XXX−XXX

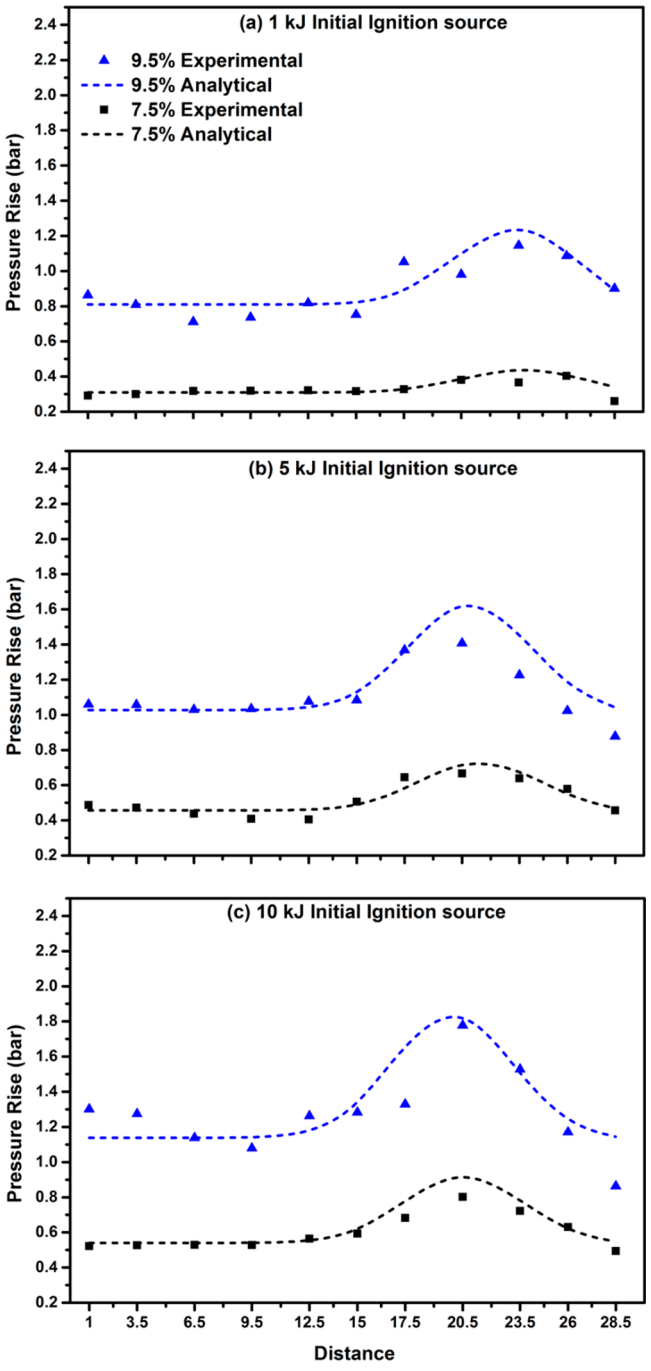

Figure 8. Pressure wave profiles for explosions of 7.5% and 9.5% methane concentrations with variable initial ignition energies of (a) 1 kJ, (b) 5 kJ, and (c) 10 kJ.

$$y = ax_i^b \tag{3}$$

where y is either y_o, A, or xc, x_i is the initial ignition energy in kJ, and a and b are constants as shown in Table 3.

Figure 8 shows the analytical and experimental results for the pressure waves for different methane concentrations as well as for different initial ignition energies. As observed, and irrespective of some slight fluctuations, the pressure waves follow similar trends for different ignition energies along the tube. The peak pressure was reached at a distance between 17.5 and 23.5 m from the ignition source. This behavior can be attributed not only due to variations in ignition energy,

Table 3. a and b Values for Eq 3

	a		b	
	7.5%	9.5%	7.5%	9.5%
y_o	0.30954	0.81012	0.24184	0.14747
xc	23.65897	23.25719	0.06179	0.06674
A	0.69907	2.34497	0.4785	0.22024

methane concentration, reactive section length, and the flame deflagration characteristics, but also to a great extent it depends on the configuration of the FDT. The unique cylindrical geometry of the FDT, with a front end closed configuration, accelerates the flame deflagration beyond the boundary where the fuel presents. Upon ignition the flame travels toward the open end of the tube, compressing the unburned gases in front of it and expanding the burned fuel behind. The turbulence caused by this relatively quick expansion and compression leads to diffusion of the flame and fuel product further into the nonreactive zone, which causes an increase in the pressure ahead of the flame front. Typically, the pressure rise continued until reaching the state of deflagration detonation transition (DDT). However, Figure 8 shows there is a significant decline in the pressure just after 26 m until the end of the FDT. This fact is not only the result of fuel consumption, but also the result of venting the compressed pressure wave ahead of the flame through the open end of the FDT, and the tendency of pressure to equalize with atmospheric pressure. Also, the reduction in pressure causes a reduction in the temperature of unburned fuel and reduces the burning rate of the front flame. Eventually, the pressure rise at the end of the FDT is reduced to minimum values. Table 4 summarizes the minimum and maximum pressure rise values that receded for 7.5% and 9.5% methane concentrations. For the 7.5% methane concentration, the pressure wave traveled in the range of 0.26 to 0.4 bar when a 1 kJ IIE was used. However, the pressure wave reading was in the range of 0.4 to 0.67 bar when a 5 kJ IIE was used. The values of the traveling pressure waves were in the range of 0.49 to 0.8 bar using a 10 kJ IIE (see Table 4).

3.2.2. Pressure Wave Velocities. The analysis of methane explosions in pipes is usually reported as a maximum pressure rise. However, it is also important to include the rise time and velocity of the pressure wave.[45] The pressure wave velocities of the 7.5% and 9.5% methane concentrations with 1, 5, and 10 kJ ignitor energies are shown in Figure 9. The pressure wave velocity was calculated from the reading of the pressure transducers at each spool. The pressure wave arrival time was considered when the pressure transducers indicated a pressure rise of 3% above the atmospheric pressure. Figure 9a shows the pressure wave velocities of the 7.5% and 9.5% methane concentrations initiated by a 1 kJ IIE.

The pressure wave velocities of both of the concentrations gradually increased until the end of the FDT. The maximum pressure wave velocity recorded was 129.8 $m \cdot s^{-1}$ and 89 $m \cdot s^{-1}$ for the 9.5% and 7.5% methane concentrations, respectively. The pressure wave significantly increased when using a 5 kJ IIE instead of the 1 kJ IIE (see Figure 9b), whereas the maximum velocity at the stoichiometric methane concentration increased 2-fold, and it increased by 45% for the 7.5% methane concentration. However, the pressure wave velocities increased by 177% and 225% for the 9.5% and 7.5% methane concentrations when using a 10 kJ energy ignitor instead of a 1 kJ ignitor (see Figure 9c). The pressure wave velocity mainly depends on the pressure wave and the pressure rise rate.

DOI: 10.1021/acs.energyfuels.6b03375
Energy Fuels XXXX, XXX, XXX−XXX

Table 4. Minimum and Maximum Values of the Pressure Rises along the FDT

		initial ignition energy (IIE)					
		1 kJ		5 kJ		10 kJ	
methane concentration		pressure rise (bar)	distance (m)	pressure rise (bar)	distance (m)	pressure rise (bar)	distance (m)
7.5%	min Pr.	0.26	28.5	0.406	12.5	0.49	28.5
	max Pr.	0.4	26	0.667	20.5	0.8	20.5
9.5%	min Pr.	0.89	28.5	0.87	28.5	0.86	28.5
	max Pr.	1.16	23.5	1.4	20.5	1.78	20.5

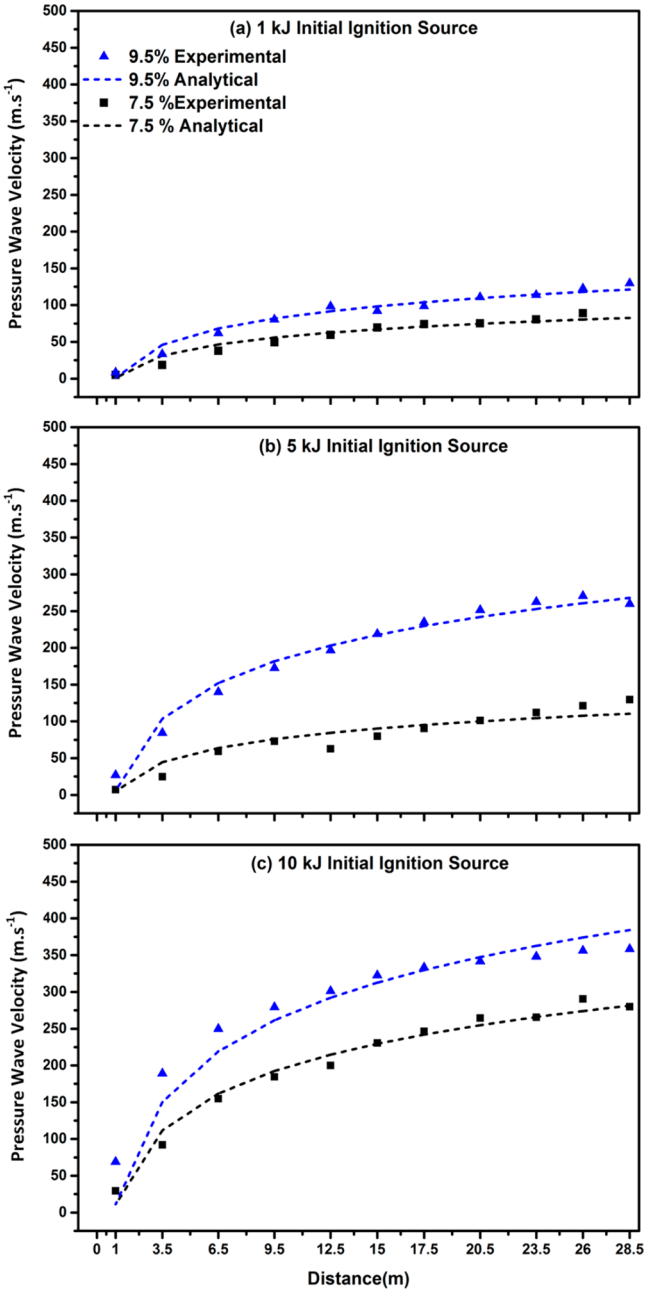

Figure 9. Pressure wave velocities for explosions of 7.5% and 9.5% methane concentrations at IIE of (a) 1 kJ, (b) 5 kJ, and (c) 10 kJ.

Presented data in Figure 9 indicate that at a 7.5% methane concentration the pressure wave velocity is significantly influenced by higher ignition energy rates (10 kJ rather than 5 kJ). The pressure wave velocity was enhanced by 45% and 225% for 5 kJ and 10 kJ ignitors, respectively. Therefore, an explosion triggered by a higher initial ignition energy has a greater tendency to produce a faster flame deflagration, and consequently a larger pressure wave rise and velocity. For the near stoichiometric methane concentrations (9.5%), however, the pressure wave velocity is significantly enhanced by approximately 100% as the initial ignition energy increases from 1 kJ to 5 kJ. It is enhanced by 117% as the initial ignition energy is increased from 1 kJ to 10 kJ (it is increased by only 17% when the ignition energy increases from 5 kJ to 10 kJ). The low relative enhancement for 9.5% as compared to 7.5%, as the IIE increases from 5 kJ to 10 kJ, could be explained as follows; the type of ignitors that are used are chemical ignitors, and their higher ignition energy consume more oxidants.[27] As the 9.5% rate is near the stoichiometric concentration, the impact of oxidant and/or fuel consumption is more noticeable. In the case of 7.5% methane concentration, there is an excess of oxidant, and the role of oxidant consumption is not a critical factor behind enhancing the burning rate, due to the increase in the initial ignition energy.

An analytical approach was developed to predict the pressure wave velocity in relation to methane concentration, ignition energy, and distance. The mathematical formula is expressed as follows:

$$P_{wv} = a_1 - b_1 \ln\left(x + \frac{\phi}{100}\right) \tag{4}$$

where P_{wv} is the pressure wave velocity, x is the distance from the ignition source (m), a_1 is the initial ignition energy in kJ, b_1 is the equation constant as seen in Table 5, and ϕ is the stoichiometric ratio which is equal to the concentration of methane in volume percent per stoichiometric concentration, as per the following equation:

$$\phi = \frac{\mathrm{MC}\%}{9.5\%} \tag{5}$$

where MC is the methane concentration.

Table 5. Constant Values (b_1) for Eq 4

	methane conc.	
initial ignition energy (kJ)	9.50%	7.50%
1	−35.9	−24.36
5	−78.5	−31.47
10	−111.7	−81.04

3.3. Flame Tracking. The flame tracking in the current work was extrapolated into two aspects; the flame intensity and the flame velocity. Calculating the flame intensity is essential to determine the lowest possible intensity that could be present during a flame's development; hence, this data will assist in integrating fire and explosion prevention in pipes and tunnels.

DOI: 10.1021/acs.energyfuels.6b03375
Energy Fuels XXXX, XXX, XXX−XXX

The flame's intensity is detailed for each run according to the IIE and the methane concentration.

3.3.1. Flame Intensity Signal. Figure 10 shows the flame intensity signals of the 7.5% and 9.5% methane concentrations

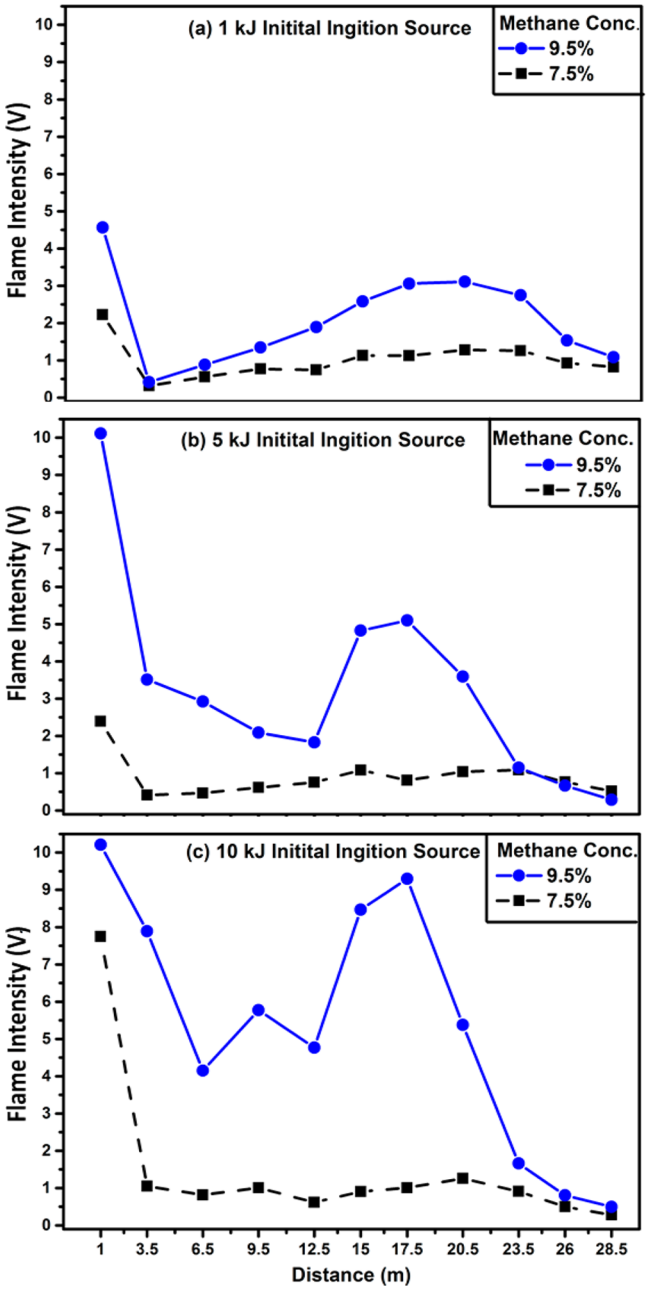

Figure 10. Flame intensities for explosions of 7.5% and 9.5% methane concentrations with IIE of (a) 1 kJ, (b) 5 kJ, and (c) 10 kJ.

ignited by 1, 5, and 10 kJ, respectively. The results reveal that there were two peaks in the flame's intensity signal along the FDT. The first peak was always located in the first chamber, and was attributed to the methane ignition around the ignitors. The second peak was attributed to the development of the flame, which is characterized by the flame's velocity. The value of these peaks, however, was dependent on the methane concentration and the IIE. Figure 10a shows the flame intensity of the methane deflagration initiated by a 1 kJ IIE. The flame intensity of the 9.5% methane concentration was higher than for the 7.5% concentration along the tube. On two occasions (at 3.5 and 28.5 m distance), however, the flame intensity curve of the 9.5% methane concentration was contiguous to the curve of the 7.5% concentration. This contiguous phenomenon indicated that the flame developed in two stages. The first stage of the flame's development started with the ignitor's ignition and diminished at 3.5 m. The second stage of development started at 3.5 m, and reached maximum flame intensity at 20.5 m, then diminished as a result of consuming the fuel. This behavior was matched for both methane concentrations. Figure 10b shows the flame intensity of the methane deflagration initiated by a 5 kJ IIE. The two stages of the flame intensity's development are obvious; where the first stage starts at ignition and diminishes at 3.5 m, and where the second stage starts (for the 7.5% methane concentration). In contrast, for the 9.5% methane concentration, the flame intensity remained low until the minimum value was reached at 12.5 m. Later, the flame intensities of both methane concentrations started the next stage, and reached their maximum within 5 m. It sharply increased to a maximum within 5 m. Finally, the lowest value of flame intensity was recorded at 28.5 m for both methane concentrations (after considering the consumption of the fuel). Figure 10c shows the flame intensity of the methane deflagration initiated by a 10 kJ IIE. The flame intensity of the 9.5% methane deflagration duly dropped to about 4.45 V at distances of 6.5 m in both stages, and the flame started to develop into the next stage at about 9.5 m. The maximum flame intensity (9.2 V) of the second stage was observed at 17.5 m. The first stage of the 7.5% methane deflagration started with a higher flame intensity, as compared to the 7.5% methane deflagration ignited by either the 1 kJ or the 5 kJ ignitors. The flame deflagrated with a flame intensity in the range of 0.6 to 1.2 V until reaching 26 m, where the flame diminished. To sum up, the flame intensities showed that the IIE has a pivotal impact on the flame deflagration. The influences were extrapolated from the intensity of the flame deflagration along the FDT. Additionally, the impacts of the IIEs are more conspicuous for the 9.5% methane concentration than for the 7.5% concentration. In all the cases of methane deflagration in this study, the flame intensity showed that the flame deflagrates in two stages. The first stage starts at the ignition source and finishes after a distance of 3.5 to 12.5 m, depending on the IIE and methane concentration.

Increasing the IIE from 1 kJ to 5 kJ caused a boost in the flame's intensity in the first stage, from 4.5 to 10 V (the maximum value of the photodiode range). Using a 10 kJ IIE instead of 5 kJ boosted the flame's intensity signal in the first stage much more, whereas the flame intensity at 3.5 m increased from 3.5 to 7.8 V. The maximum value of flame intensity in the second stage was also affected by the IIE, whereas the values increased from 3.1 to 5.1 V, then to 9.2 V, as the IIE was increased from 1 kJ to 5 kJ, then to 10 kJ. For the deflagration of the 7.5% methane concentration, the flame intensity in the first stage was more sensitive to the 10 kJ IIE than to the 1 kJ IIE. There were no significant changes in the flame intensity as the IIE was increased from 1 kJ to 5 kJ. The flame intensity in the first stage, however, significantly increased from about 2.5 to 7.8 V as the IIE was increased from 5 kJ to 10 kJ. Finally, in the second stage for the 7.5% methane concentration, the IIE did not have a significant impact on the flame intensity.

3.3.2. Flame Velocity. The characteristics of the pressure waves discussed previously (see Section 3.2), are mainly

DOI: 10.1021/acs.energyfuels.6b03375
Energy Fuels XXXX, XXX, XXX−XXX

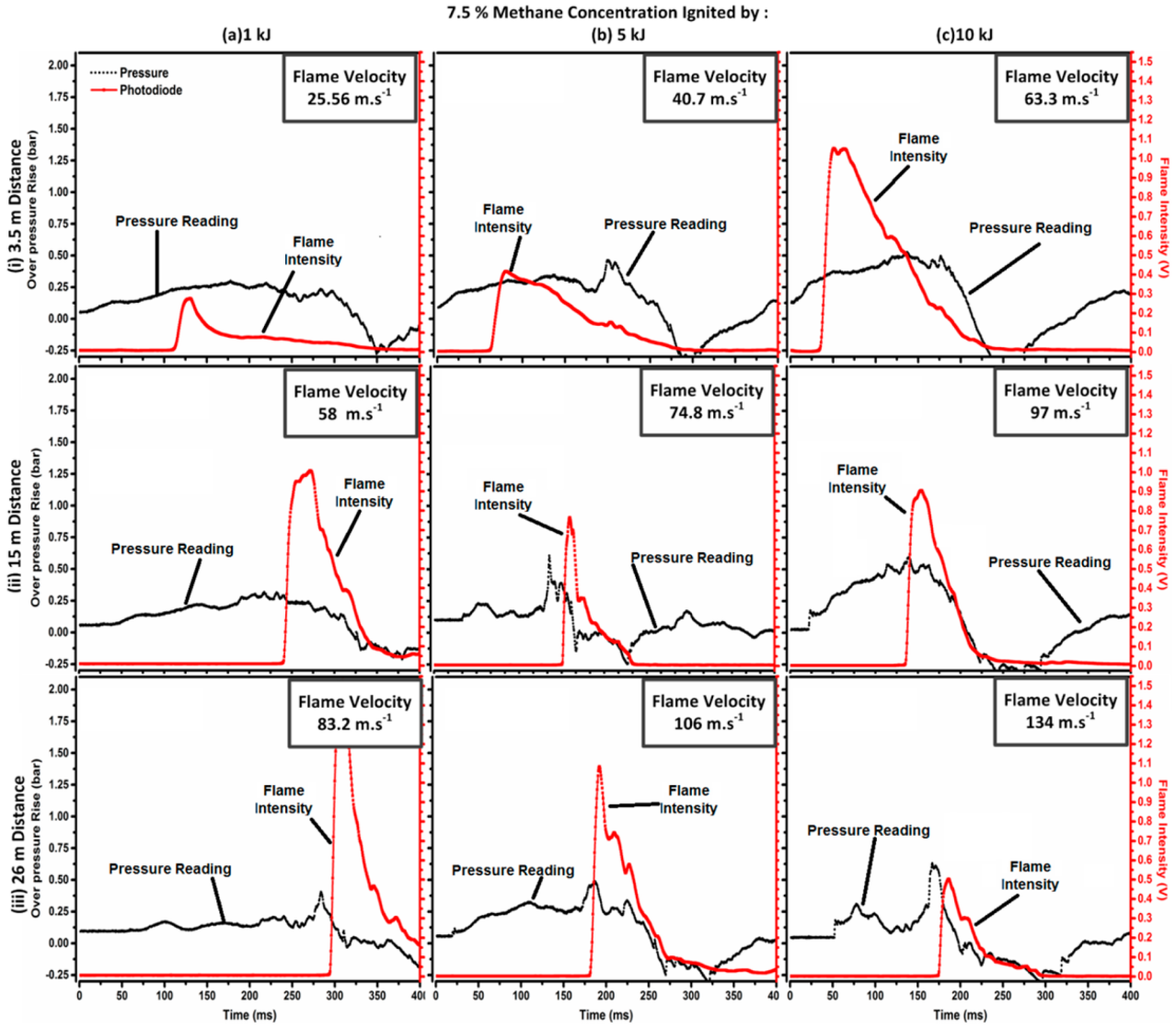

Figure 11. Flame velocities, pressure rise profiles, and flame intensity signal profiles over time for 7.5% methane concentrations ignited by (a) 1 kJ, (b) 5 kJ, and (c) 10 kJ at distances of (i) 3.5 m, (ii) 15 m, and (iii) 26 m.

dependent on how fast the flame deflagrates in the FDT.[46,47] Hence, the consequences of explosions in pipes depend on the velocity of the flame deflagration.[45,48] The determination of a flame's velocity is mainly dependent on the burning rate and the velocity of the gases just ahead of the flame.[49−51] It has been proven that the ignition energy can influence the measurement of the burning rate.[52] In this section, the methane flame deflagration velocity is investigated for 7.5% and 9.5% methane concentrations and three different IIEs, which were 1, 5, and 10 kJ. The flame velocity was calculated from the photodiode's readings. When the photodiode signal reached 0.3 V the flame was considered to have reached to that sensor location and this arrival time was used to calculate the flame velocity. Then the flame front velocity can be calculated relative to the ignition point. The flame deflagration velocities, and the pressure wave development of an explosion at a 7.5% methane concentration, are illustrated in Figure 11. The figure details the relation between the flame deflagrations and the IIE, for energies of 1 kJ (Figure 11a), 5 kJ (Figure 11b), and 10 kJ (Figure 11c), and the distances from the ignition source of 3.5 m (Figure 11i), 15 m (Figure 11ii), and 26 m (Figure 11iii). The data shows that the IIE significantly impacted on the flame deflagration velocities at varying distances along the tube.

The flame velocity of a methane explosion initiated by a 1 kJ IIE at 3.5 m, shown in Figure 11a (i), increased 2-fold when the velocity measurement location from the ignition source was increased to 15 m, as shown in Figure 11a (ii). The flame deflagration velocity continued to develop until it reached the end of the tube, recording 83.2 $m \cdot s^{-1}$ at 26 m (Figure 11a (iii)). The figure clearly shows that the development of the flame deflagration velocity between 3.5 and 15 m distance was much faster than for the distance between 15 and 26 m. The flame velocities of the methane explosions along the FDT for a 5 kJ ignitor at 3.5 m (Figure 11b (i)) and 26 m (Figure 11b (iii)) were enhanced, as compared to a 1 kJ ignitor at the same distances (Figure 11a (i) and Figure 11a (iii)), increasing by 15 $m \cdot s^{-1}$ and 23 $m \cdot s^{-1}$, respectively. The high speed camera images (Figure 13a) showed that the front flame of the methane ignited by a 1 kJ ignitor was slower than the front flame of a 5 kJ ignitor methane explosion by about 35 ms. It was also observed that at that distance there was no fireball for the methane flame deflagrations. However, for the methane

DOI: 10.1021/acs.energyfuels.6b03375
Energy Fuels XXXX, XXX, XXX−XXX

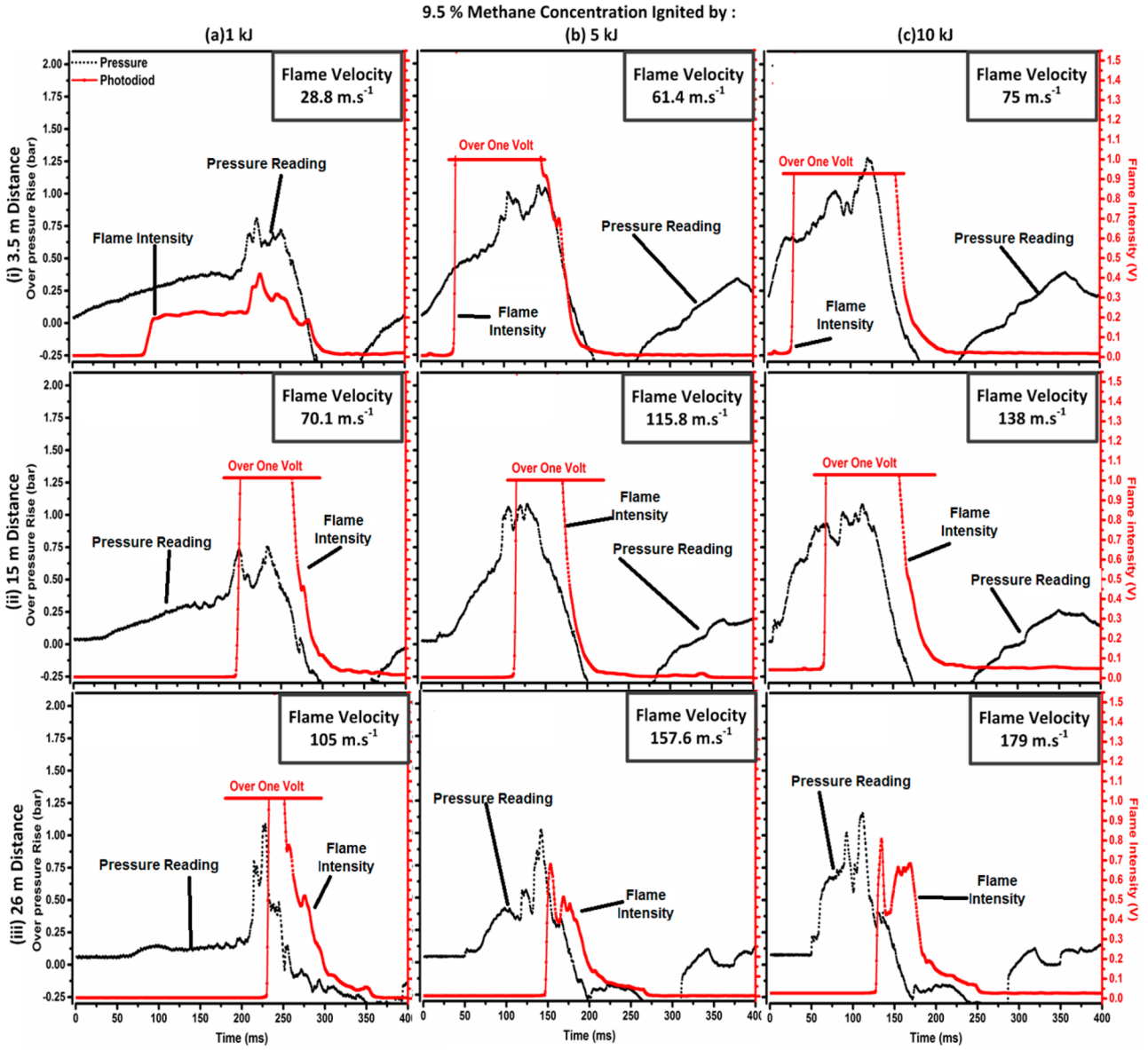

Figure 12. Flame velocities, pressure rise profiles, and flame intensity profiles over time for 9.5% methane concentrations ignited by (a) 1 kJ, (b) 5 kJ, and (c) 10 kJ at distances of (i) 3.5 m, (ii) 15 m, and (iii) 26 m.

flame deflagrations ignited by a 5 kJ ignitor, the fireball was sustained for about 10−15 ms. The flame deflagrations for the 7.5% methane concentration ignited by a 10 kJ IIE are shown in Figure 13a.

It was observed that increasing the IIE to 10 kJ enhanced the velocity of the methane flame deflagration. The flame deflagration velocity with a 10 kJ IIE at a distance of 3.5 m (Figure 11c (i)) was faster than that for 1 kJ ignitions (Figure 11a (i)) and 5 kJ ignitions (Figure 11b (i)) by about 38 $m{\cdot}s^{-1}$ and 22 $m{\cdot}s^{-1}$, respectively. The high speed camera images showed that the methane flame front ignited by a 5 kJ ignitor was slower than the flame front of a 10 kJ ignitor by about 15 ms. The images of the 10 kJ ignitor methane explosions also showed that the time delay between the fire ball and the flame front was less than 3 ms, as compared to about 10 ms for a 5 kJ ignitor (see Figure 13b).The flame deflagration velocity and pressure wave development of an explosion for the 9.5% methane concentration are shown in Figure 12. The influence of the IIE in enhancing the flame deflagration velocity along the FDT was obvious. The deflagration velocity was more enhanced for the 9.5% methane concentration than for the 7.5% concentration. For example, the percentage increase in the flame deflagration velocity (enhancement ratio) when implying a 10 kJ IIE (Figure 12a (i)) rather than a 1 kJ IIE (Figure 12c (i)) was about 165% for the 9.5% methane concentration, as compared to 147% for the 7.5% concentration at a distance of 3.5 m (Figure 11a (i) and Figure 11c (i)). Indeed, it was observed that the rate of the flame deflagration's velocity development along the FDT for a low ignition energy was greater than the velocity from a high ignition energy, where the enhancement ratio of the flame velocities from the distance of 3.5 to 26 m was 265, 156, and 138%, respectively, for the 1, 5, and 10 kJ IIE (see Figure 12a (iii), Figure 12b (iii), and Figure 12c (iii)). The lower flame velocity enhancement ratio for the higher IIE can be attributed to the fact that the burning rate of the methane at the first distance, when implying a higher IIE, was much higher than when implying a low IIE. Also, the high consumption of methane due to the high burning rate at 3.5 m

DOI: 10.1021/acs.energyfuels.6b03375
Energy Fuels XXXX, XXX, XXX−XXX

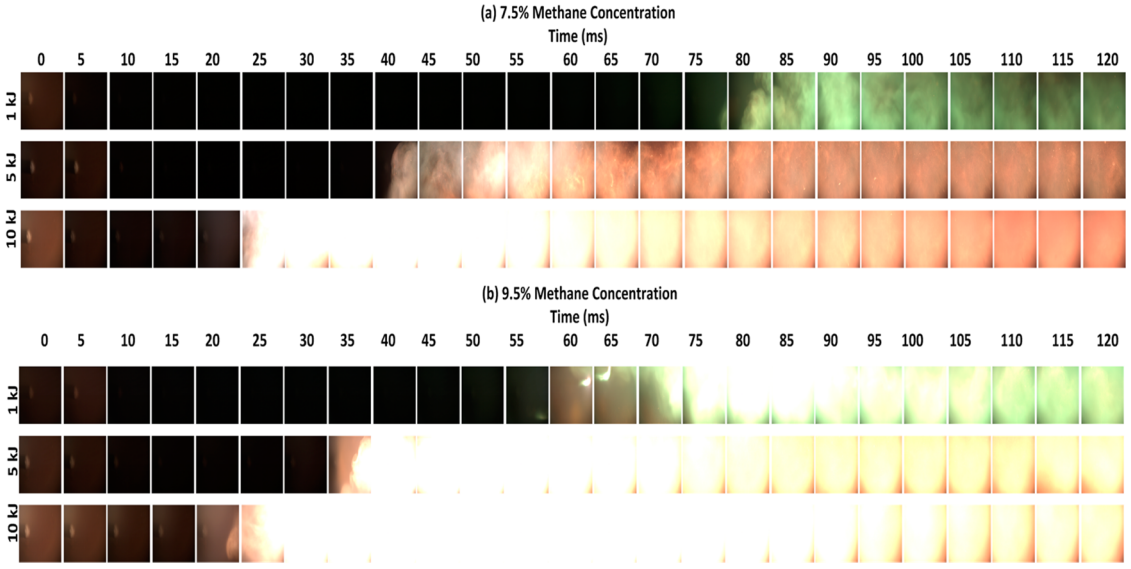

Figure 13. Images of deflagration of methane ignited by 1, 5, and 10 kJ IIE for (a) 7.5% methane concentration (b) 9.5% methane concentration.

resulted in reducing the methane concentration at the 28.5 m mark, and eventually reducing the flame enhancement velocity ratio. Unlike the flame deflagration for the 7.5% methane concentration, a visual fireball was observed when the 9.5% methane mixture was ignited by a 1 kJ IIE (Figure 13b) and the fireball followed about 10 ms behind the flame front. The fireballs of the methane deflagrations initiated by 5 kJ and 10 kJ IIE were only a few milliseconds behind the flame front (see Figure 13a). Finally, the time of the fireball's appearance was significantly affected by the IIE. The fireball for the 7.5% methane concentration with a 5 kJ IIE appeared for about 10 ms, as compared to 50 ms when implying a 10 kJ IIE (Figure 13a). There was no fireball observed when a 1 kJ IIE was used. The fireball for the 9.5% methane concentration lasted for a greater length of time for both 5 kJ and 10 kJ IIE, lasting for 50 and 75 ms, respectively (see Figure 13b).To sum up, the IIE energy has a pronounced influence on the deflagration velocity. For the 7.5% methane concentration, by increasing the energy of the IIE by 5 times (1 kJ to 5 kJ), the flame deflagration velocity increased by about 59%, and increasing the initial IIE from 1 kJ to 10 kJ enhanced the flame deflagration velocity by 147%.

The flame deflagrated to the end of the FDT and the velocity continually accelerated. The flame reached 26 m with an enhancement ratio of about 225, 160, and 111%, respectively, for the 1, 5, and 10 kJ IIE. Finally, the sensitivity of the methane flame's deflagration velocity to the IIE was far more obvious for the 9.5% methane concentration, as compared to the 7.5% methane concentration. The enhancement ratios of the 5 kJ and 10 kJ IIE energies at a distance of 3.5 m were 160% and 160% for the 9.5% methane concentration, and 59% and 147% for the 7.5% methane concentration, respectively. For 5% methane, no flame was detected when 1 kJ and 5 kJ ignitors were used, however, for the 10 kJ ignitor a small flickering flame was observed. The flame was detected at 1 m distance from the ignitor at a velocity of 3.74 $m \cdot s^{-1}$ with a flame intensity signal of 0.32 V.

Table 1and Figure 14 provide summaries of the most relevant research findings available in the open literature. The outcomes of the current study indicate a relatively good agreement with the previous studies by scholars, such as Ajrash et al. 2017.[34] Perhaps the experimental work which is closest to this study belongs to Wei et al.[11] They employed an FDT with dimensions similar to the FDT in this study and obtained a pressure rise of 2.3 for a 9.5% methane concentration. However, no data for flame velocity or pressure wave behavior was reported, and neither was the ignition source configuration clarified. Jiang et al.[41] also employed an FDT, but the cross sectional area was less than the FDT of this work, which resulted in lowering the value of the maximum pressure rise. Liu et al.[43] used a high initial ignition energy which could lead to a detonation, however, no further information regarding the flame deflagration could be extrapolated from his work. To sum up, employing high ignition energies, lab scale, and fully confined apparatuses do not provide accurate data for flame deflagration and its consequences, which may occur in the extractive and other interconnected industries, where fugitive methane is emitted from underground coal mines.

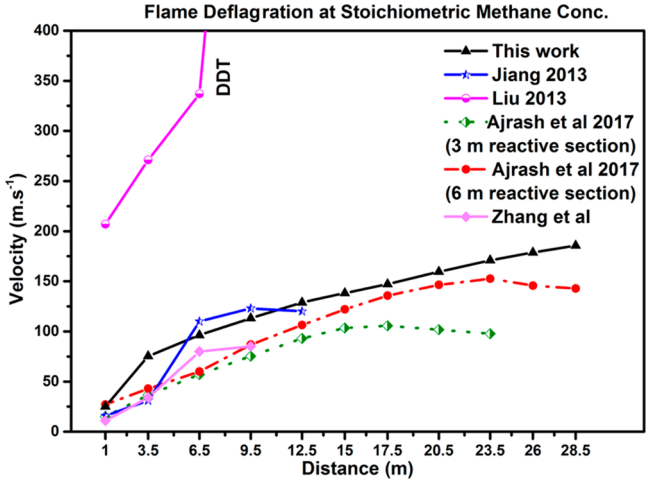

Figure 14. Comparison of flame deflagration of this work with flame deflagration according to literature review.

4. CONCLUSION

The influences of initial ignition energy on flame deflagration properties were investigated in a flame deflagration tube. Three

DOI: 10.1021/acs.energyfuels.6b03375
Energy Fuels XXXX, XXX, XXX−XXX

energies were used as IIE, which were 1, 5, and 10 kJ. The conclusions can be summarized as follows:

- Methane concentration at 5% does not form flame deflagration in an axial direction from the duct unless ignited by an initial ignition energy of at least 10 kJ.
- Increasing the IIE to 10 kJ increased the maximum pressure rises by 45% and 56% for methane concentrations of 7.5% and 9.5%, respectively.
- The stagnation pressure at the end of the tube also showed sensitivity to the IIE, where for the 7.5% methane concentration, the stagnation pressures increased by 35% and 58%, respectively, when the initial ignition energy was increased from 1 kJ to 5 kJ, and from 1 kJ to 10 kJ. For the 9.5% methane concentration, the stagnation pressures increased by 14% and 25% as the initial ignition energy was increased from 1 kJ to 5 kJ, and to 10 kJ, respectively.
- The pressure wave profile showed that the pressure wave traveled at an almost constant pressure. Then, at a specific distance, the pressure rose to a certain pressure, depending on the IIE and the methane concentration. The data revealed that the pressure wave developed for a 9.5% methane concentration starts at a distance of 15 m from the ignition point for 1 kJ and 5 kJ IIE. For the 7.5% methane concentration, however, the pressure wave peak was less obvious, especially when 1 kJ was used as the IIE. Increasing the IIE from 1 kJ to 5 kJ, or to 10 kJ, increased the value of the peak pressure and it became more distinct at distances between 15 and 26 m. Moreover, the maximum pressure wave velocity for the 9.5% methane concentration dramatically tripled as the IIE was increased from 1 kJ to 10 kJ.
- The flame intensity conventionally showed two courses of rise along the flame deflagration tube. The first course emerged at the location of initial ignition and the second peak developed after a distance of 12.5 m. The intensity signal of the flame in both courses was significantly affected by the energy of the IIE. Also, the highest flame intensity of the second course appeared 3 m earlier when using a 5 kJ or 10 kJ IIE instead of a 1 kJ. For the 7.5% methane concentration, the flame intensity of the first course was less affected by the IIE than it was for the 9.5% methane concentration. When increasing the IIE from 1 kJ to 5 kJ, no notable change was recorded in the flame intensity along the tube.
- The first outcome to be observed regarding the flame velocity was that the flame deflagration velocities continually increased during the course of the flame deflagration tube. The flame deflagration velocity showed a direct proportional relationship to the IIE. For example, when the IIE was increased 5 times, the flame deflagration velocities increased by 27.4% and 50%, respectively, for the 7.5% and 9.5% methane concentrations. Finally, when the IIE was increased 10 times, the flame deflagration velocities increased by 61% and 70%, respectively, for the 7.5% and 9.5% methane concentrations.
- More reliable data can extracted from the flame deflagration tube when it has an open end, which eliminates the interaction of the reflection wave with the front flame. Employing a relatively low ignition energy also results in more reliable data. The pressure wave values and the pressure wave velocities can be analytically solved depending on the methane concentration, energy of ignition, and the distance with an average error of 7.5%.

AUTHOR INFORMATION

Corresponding Author

*E-mail: jafar.zanganeh@newcastle.edu.au.

ORCID

Jafar Zanganeh: 0000-0002-7112-2246

Behdad Moghtaderi: 0000-0002-9409-4225

Notes

The authors declare no competing financial interest.

ACKNOWLEDGMENTS

The researcher would like to acknowledge the financial support provided to this project by Australian Coal Association Low Emission Technologies Ltd (ACALET), the Australian Department of Industry, and the University of Newcastle, Australia. In addition, special gratitude is given to the Higher Committee for Education Development (HCED) from the Iraqi government and the Midland Refineries Company (MRC) for sponsoring a postgraduate candidate to work on this project.

REFERENCES

(1) Kundu, S.; Zanganeh, J.; Moghtaderi, B. A Review on Understanding Explosions from Methane-Air Mixture. *J. Loss Prev. Process Ind.* **2016**, *40*, 507−523.

(2) Zhang, B.; Pang, L.; Gao, Y. Detonation limits in binary fuel blends of methane/hydrogen mixtures. *Fuel* **2016**, *168*, 27−33.

(3) van Rooyen, G. Ignition and initiation of coal mine explosions. Ph.D Thesis, University of the Witwatersrand, 1992.

(4) Pekalski, A.; Puttock, J.; Chynoweth, S. Deflagration to detonation transition in a vapour cloud explosion in open but congested space: Large scale test. *J. Loss Prev. Process Ind.* **2015**, *36*, 365−370.

(5) Lees, F. *Loss Prevention in the Process Industries: Hazard Identification, Assessment and Control*; Butterworth-Heinemann, 2012.

(6) Abel, F. Contributions to the History of Explosive Agents. *Philos. Trans R Soc. London.* **1869**, *159*, 489−516.

(7) Mallard, E.; Le Chatelier, H. Sur les vitesses de propagation de l'inflammation dans les me langes gazeux explosifs. *CR Ac des Sc.* **1881**, *93*, 145−148.

(8) Mason, W.; Wheeler, R. V. The "uniform movement" during the propagation of flame. *J. Chem. Soc., Trans.* **1917**, *111*, 1044−1057.

(9) Mason, W.; Wheeler, R. V. The propagation of flame in mixtures of methane and air. Part I. Horizontal propagation. *J. Chem. Soc., Trans.* **1920**, *117* (0), 36−47.

(10) Phylaktou, H.; Andrews, G.; Herath, P. Fast flame speeds and rates of pressure rise in the initial period of gas explosions in large L/D cylindrical enclosures. *J. Loss Prev. Process Ind.* **1990**, *3*, 355−364.

(11) Wei, H., Gillies, W.A.D.S., Oberholzer, J. W., Davis, R. Australian Sealing Practice and use of Risk Assessment Criteria - ACARP Project C17015. In: *In Proceedings of the Queensland Mining Industry Health and Safety Conference*; Queensland, Australia, 2009; pp 23−26.

(12) Li, Q.; Lin, B.; Jian, C. Investigation on the Interactions of Gas Explosion Flame and Reflected Pressure Waves in Closed Pipes. *Combust. Sci. Technol.* **2012**, *184* (12), 2154−2162.

(13) Oran, E. S.; Gamezo, V. N.; Zipf, R. K. Large-Scale Experiments and Absolute Detonability of Methane/Air Mixtures. *Combust. Sci. Technol.* **2015**, *187* (1−2), 324−341.

(14) Gamezo, V. N.; Zipf, R. K.; Sapko, M. J.; et al. Detonability of natural gas-air mixtures. *Combust. Flame* **2012**, *159* (2), 870−881.

DOI: 10.1021/acs.energyfuels.6b03375
Energy Fuels XXXX, XXX, XXX−XXX

(15) Oran, E. S.; Gamezo, V. N.; Kessler, D. A. *Deflagrations, Detonations, and the Deflagration-to-Detonation Transition in Methane-Air Mixtures*; 2011.
(16) Gelfand, B. E.; Khomik, S. V.; Bartenev, A. M.; Medvedev, S. P.; Olivier, H.; Gronig, H. Detonation and deflagration initiation at the focusing of shock waves in combustible gaseous mixture. *Shock Waves.* **2000**, *10* (3), 197−204.
(17) Bull, D. C.; Elsworth, J. E.; Shuff, P. J.; Metcalfe, E. Detonation cell structures in fuel/air mixtures. *Combust. Flame* **1982**, *45* (C), 7−22.
(18) Wolanski, P.; Kauffman, C. W.; Sichel, M.; Nicholls, J. A. Detonation of methane-air mixtures. *Symp. Combust., [Proc.]* **1981**, *18* (1), 1651−1660.
(19) Peraldi, O.; Knystautas, R.; Lee, J. H. Criteria for transition to detonation in tubes. *Symp. Combust., [Proc.]* **1988**, *21* (1), 1629−1637.
(20) Kuznetsov, M.; Alekseev, V.; Yankin, Y.; Dorofeev, S. Slow and fast deflagrations in Hydrocarbon-air mixtures. *Combust. Sci. Technol.* **2002**, *174* (5−6), 157−172.
(21) Carcassi, M. N.; Fineschi, F. Deflagrations of H2-air and CH4-air lean mixtures in a vented multi-compartment environment. *Energy* **2005**, *30*, 1439−1451.
(22) Shepherd, J. E. Structural Response of Piping to Internal Gas Detonation. *J. Pressure Vessel Technol.* **2009**, *131* (3), 031204.
(23) Knystautas, R.; Lee, J. H.; Guirao, C. M. The critical tube diameter for detonation failure in hydrocarbon-air mixtures. *Combust. Flame* **1982**, *48*, 63−83.
(24) Ajrash, M. J.; Zanganeh, J.; Moghtaderi, B. Fundamental Study on Coal Dust Cloud Auto Ignition and Methane Flammability Limit in Ventilation Air Methane (VAM). *IJRCMCE* **2015**, *2*, 118−121.
(25) Tieszen, S.; Pitz, W.; Stamps, D. W.; Westbrook, C. K. Gaseous Hydrocarbon-Air Detonations. *Combust. Flame* **1991**, *84*, 376−390.
(26) Zabetakis, M. G. *Flammability Characteristics of Combustible Gases and Vapors*; 1965.
(27) Hertzberg, M.; Cashdollar, K. L.; Zlochower, I a. Flammability limit measurements for dusts and gases: Ignition energy requirements and pressure dependences. *Symp. Combust., [Proc.]* **1988**, *21*, 303−313.
(28) Cashdollar, K. L.; Zlochower, I. A.; Green, G. M.; Thomas, R. A.; Hertzberg, M. Flammability of methane, propane, and hydrogen gases. *J. Loss Prev. Process Ind.* **2000**, *13*, 327−340.
(29) Bai, C.; Gong, G.; Liu, Q.; Chen, Y.; Niu, G. The explosion overpressure field and flame propagation of methane/air and methane/coal dust/air mixtures. *Saf Sci.* **2011**, *49* (10), 1349−1354.
(30) Zhang, Q.; Li, W.; Liang, H. Effect of spark duration on explosion parameters of methane/air mixtures in closed vessels. *Saf Sci.* **2012**, *50* (9), 1715−1721.
(31) Ajrash, M. J.; Zanganeh, J.; Moghtaderi, B. Effects of ignition energy on fire and explosion characteristics of dilute hybrid fuel in ventilation air methane. *J. Loss Prev. Process Ind.* **2016**, *40*, 207−216.
(32) Ajrash, M. J.; Zanganeh, J.; Moghtaderi, B. Methane-coal dust hybrid fuel explosion properties in a large scale cylindrical explosion chamber. *J. Loss Prev. Process Ind.* **2016**, *40*, 317−328.
(33) Ajrash, M. J.; Zanganeh, J.; Moghtaderi, B. Deflagration of Premixed Methane-Air in a Large Scale Detonation Tube. *Process Saf. Environ. Prot.* **2017**, DOI: 10.1016/j.psep.2017.03.035.
(34) Ajrash, M. J.; Zanganeh, J.; Moghtaderi, B. The flame deflagration of hybrid methane coal dusts in a large-scale detonation tube (LSDT). *Fuel* **2017**, *194*, 491−502.
(35) Mitu, M.; Giurcan, V.; Razus, D.; Prodan, M.; Oancea, D. Journal of Loss Prevention in the Process Industries Propagation indices of methane-air explosions in closed vessels. *J. Loss Prev. Process Ind.* **2017**, *47*, 110−119.
(36) Tang, C.; Zhang, S.; Si, Z.; Zhang, K.; Jin, Z.; Huang, Z. High methane natural gas air explosion characteristics in confined. *J. Hazard. Mater.* **2014**, *278*, 520.
(37) Gieras, M.; Klemens, R.; Rarata, G.; Wolanski, P. Determination of explosion parameters of methane-air mixtures in the chamber of 40 dm 3 at normal and elevated temperature. *J. Loss Prev. Process Ind.* **2006**, *19*, 263−270.
(38) Kindracki, J.; Kobiera, A.; Rarata, G.; Wolanski, P. Influence of ignition position and obstacles on explosion development in methane-air mixture in closed vessels. *J. Loss Prev. Process Ind.* **2007**, *20* (4−6), 551−561.
(39) Badr, O.; Karim, G. Flame Propagation in Stratified Methane-Air Mixtures. *J. Fire Sci.* **1984**, *2*, 415−426.
(40) Cao, X.; Ren, J.; Bi, M.; Zhou, Y.; Li, Y. Experimental research on the characteristics of methane/air explosion affected by ultrafine water mist. *J. Hazard. Mater.* **2017**, *324*, 489−497.
(41) Jiang, B.; Lin, B.; Zhu, C.; Zhai, C.; Liu, Q. Premixed methane-air deflagrations in a completely adiabatic pipe and the effect of the condition of the pipe wall. *J. Loss Prev. Process Ind.* **2013**, *26* (4), 782−791.
(42) Zhang, Q.; Ma, Q. J. Dynamic pressure induced by a methane − air explosion in a coal mine. *Process Saf. Environ. Prot.* **2015**, *93*, 233−239.
(43) Liu, Q.; Hu, Y.; Bai, C.; Chen, M. Methane/coal dust/air explosions and their suppression by solid particle suppressing agents in a large-scale experimental tube. *J. Loss Prev. Process Ind.* **2013**, *26* (2), 310−316.
(44) Lees, F. Pressure System Design. *Lees Loss Prevention in the Process Industries* **2012**, 509−617.
(45) Halter, F.; Chauveau, C.; Djebaili-Chaumeix, N.; Gokalp, I. Characterization of the effects of pressure and hydrogen concentration on laminar burning velocities of methane-hydrogen-air mixtures. *Proc. Combust. Inst.* **2005**, *30* (1), 201−208.
(46) Otsuka, T.; Saitoh, H.; Mizutani, T.; Morimoto, K.; Yoshikawa, N. Hazard evaluation of hydrogen-air deflagration with flame propagation velocity measurement by image velocimetry using brightness subtraction. *J. Loss Prev. Process Ind.* **2007**, *20* (4−6), 427−432.
(47) Eckhoff, R. *Explosion Hazards in the Process Industries*; Elsevier, 2013.
(48) Bjerketvedt, D.; Bakke, J. R.; Van Wingerden, K. *Gas Explosion Handbook*; 1997; Vol *52*.
(49) Tien, J. H.; Matalon, M. On the burning velocity of stretched flames. *Combust. Flame* **1991**, *84* (3−4), 238−248.
(50) Andrews, G. E.; Bradley, D. The burning velocity of methane-air mixtures. *Combust. Flame* **1972**, *19* (2), 275−288.
(51) Zhang, M.; Wang, J.; Xie, Y.; et al. Measurement on instantaneous flame front structure of turbulent premixed CH4/H2/air flames. *Exp. Therm. Fluid Sci.* **2014**, *52*, 288−296.
(52) Huang, Z.; Zhang, Y.; Zeng, K.; Liu, B.; Wang, Q.; Jiang, D. Measurements of laminar burning velocities for natural gas-hydrogen-air mixtures. *Combust. Flame* **2006**, *146* (1−2), 302−311.

DOI: 10.1021/acs.energyfuels.6b03375
Energy Fuels XXXX, XXX, XXX−XXX